Supplementary Information

Single-step Chemical Vapour Deposition of Anti-pyramid MoS_2/WS_2 Vertical Heterostructures

Xueyin Bai,[1,*] Shisheng Li,[2] Susobhan Das,[1] Luojun Du,[1] Yunyun Dai,[1] Lide Yao,[3] Ramesh Raju,[1] Mingde Du,[1] Harri Lipsanen,[1] and Zhipei Sun[1,4]

1. Department of Electronics and Nanoengineering, Aalto University, Finland
2. International Center for Young Scientists (ICYS), National Institute for Materials Science (NIMS), Japan
3. Department of Applied Physics, Aalto University, Finland
4. QTF Centre of Excellence, Department of Applied Physics, Aalto University, Finland

E-mail: xueyin.bai@aalto.fi

Calculation of SHG intensity from second-order susceptibility

The total SHG intensity in the heterostructure with an angle between two layers, $I_h(\theta)$, is expressed as[1]

$$I_h(\theta) = I_1 + I_2 + 2\sqrt{I_1 I_2 \cos\theta} \quad (1)$$

where $I_h(\theta)$ stands for the SHG intensity in the stacking heterostructure; θ is the stacking angle, which is defined as the different angle between two stacking layers and is 60° in AA' stacking. Meanwhile, the SH intensity I is proportional to the square of polarization *P* as $I \propto P^2$. The relationship between polarization and susceptibility is[2]

$$P = \chi^{(1)}E + \chi^{(2)}E^2 + \chi^{(3)}E^3 + \cdots \quad (2)$$

where $(\chi^{(1)})$, $(\chi^{(2)})$ and $(\chi^{(3)})$ stand for linear, second-order and third-order susceptibilities, respectively; and E is the electrical field of the incident light. Hence, it can be deduced that $I \propto (\chi^{(2)})^2$ and the equation (1) can be written as

$$I_h(\theta) \propto \left(\chi_1^{(2)}\right)^2 + \left(\chi_2^{(2)}\right)^2 + 2\left|\chi_1^{(2)}\right|\left|\chi_2^{(2)}\right|\cos\theta \quad (3)$$

Optical micrograph over a wide area and a histogram of grain sizes

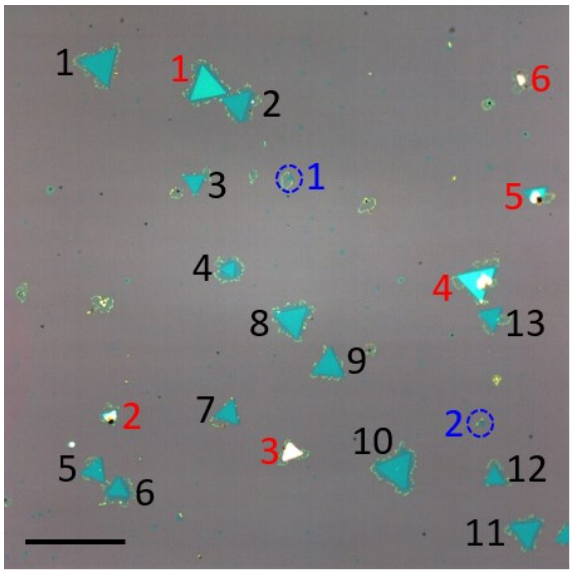

Figure S1. Optical micrograph over a wide area of MoS_2/WS_2 heterostructures (black numbers), bulk flakes (red numbers) and small monolayer WS_2 (blue numbers). Scale Bar, 100 μm.

Optical characterization of MoS_2 flakes on the substrate with Na_2MoO_4

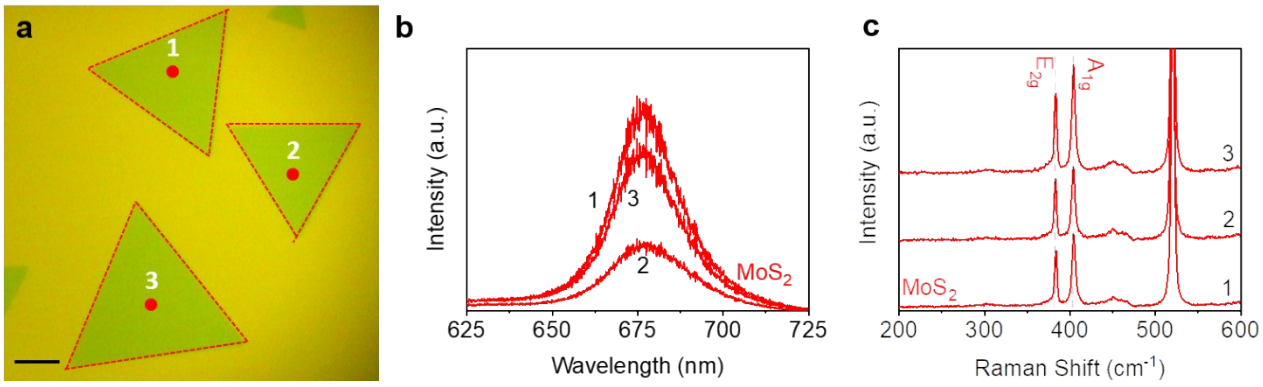

Figure S2. Optical characterization of MoS_2 flakes on the substrate with Na_2MoO_4. (a) Optical microscopy images of MoS_2 flakes (Scale Bar, 25 μm). (b) PL and (c) Raman spectra of the marked positions in (a), respectively.

AFM characterization of a typical MoS_2/WS_2 heterostructure

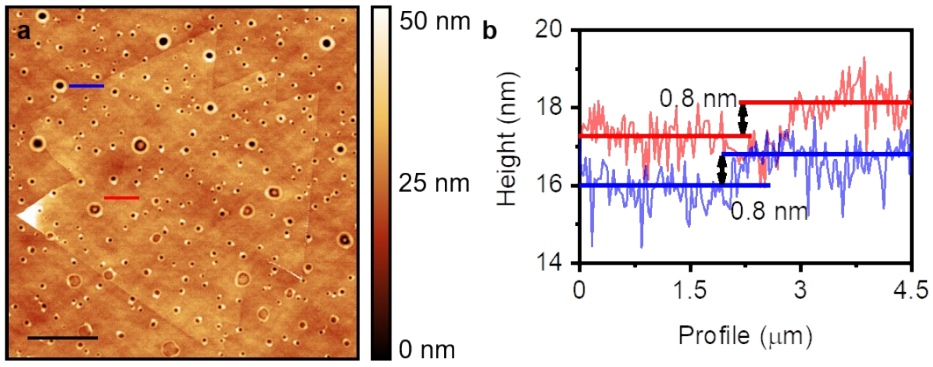

Figure S3. AFM image. (a) AFM image of MoS_2/WS_2 heterostructure (The holes are created by the etchant of sodium.[3] (Scale Bar: 10 μm). (b) the height profiles of marked lines in (a).

Statistical data of anti-pyramid heterostructures

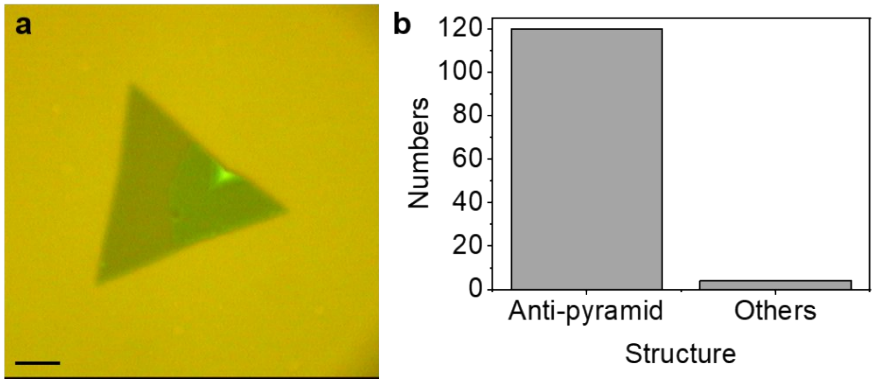

Figure S4. Statistical data of anti-pyramid heterostructures. (a) An example of a non-anti-pyramid heterostructure (Scale Bar, 10 μm). (b) Statistics of anti-pyramid heterostructures and others.

Artificial anti-pyramid MoS_2/WS_2 heterostructure

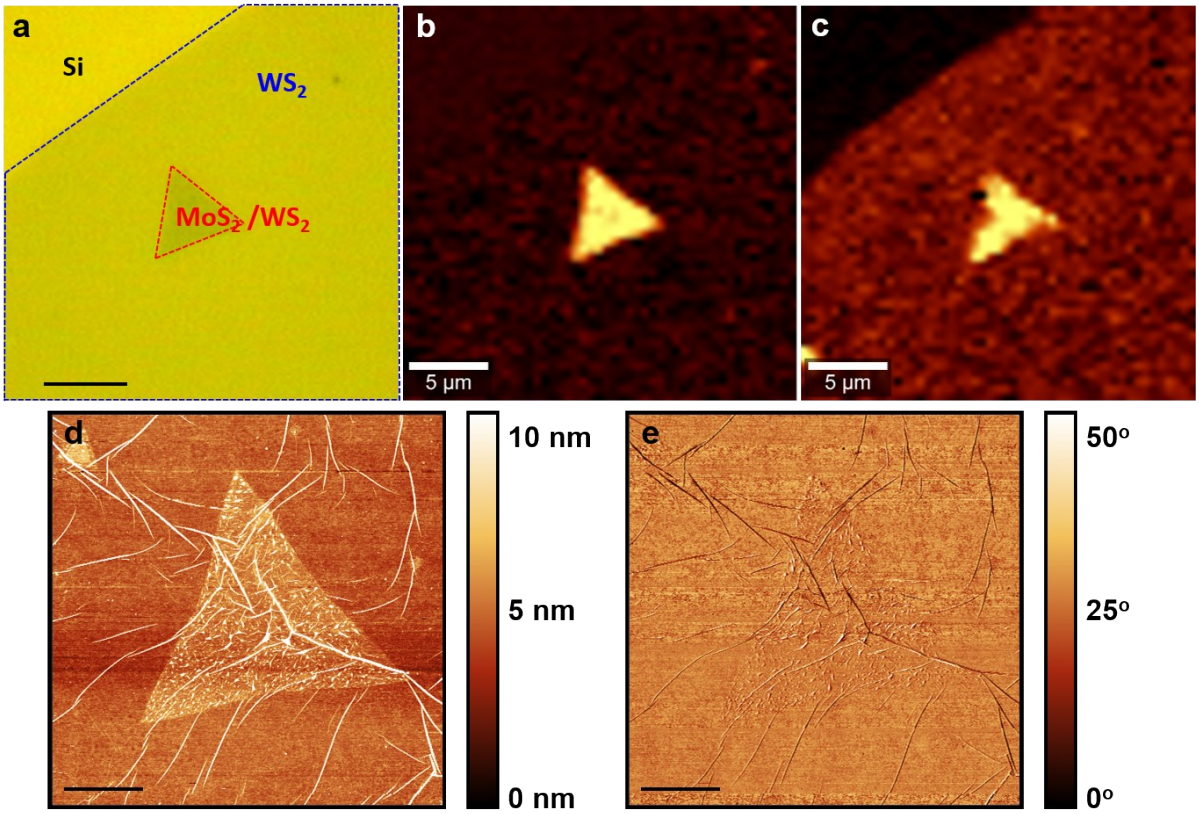

Figure S5. Artificial anti-pyramid MoS_2/WS_2 heterostructures by transferring a thin film of monolayer WS_2 on triangular flakes of monolayer MoS_2. (a) Optical image of an artificial heterostructure (Scale Bar, 5 μm). (b-c) Raman mapping at (b) 385 cm^{-1} (MoS_2) and (c) 351 cm^{-1} (WS_2) with a 532 nm laser, respectively. (d-e) AFM (d) topographic and (e) phase images.

Diffusion of precursors

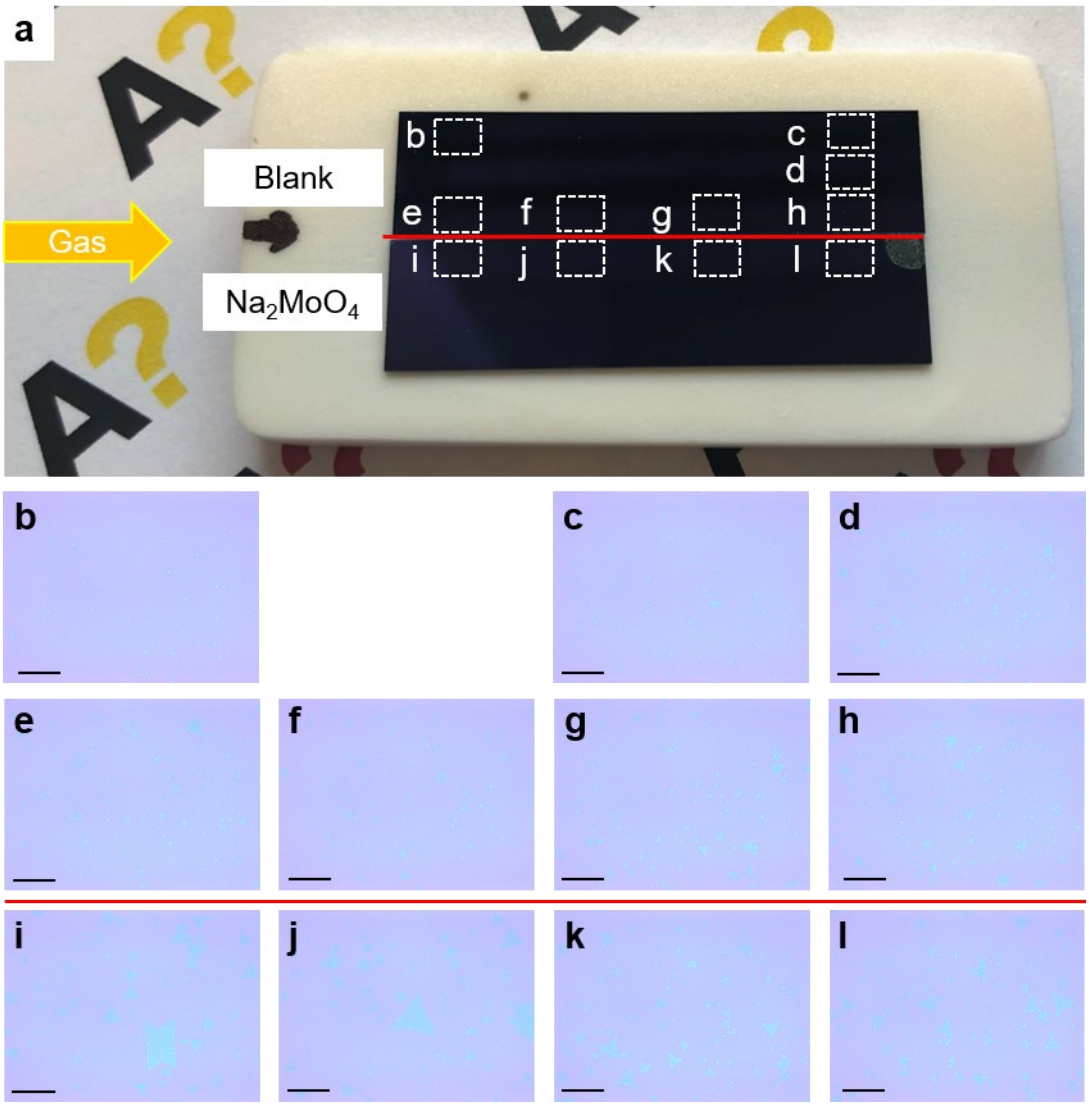

Figure S6. Control experiment of Na_2MoO_4 diffusion. (a) Photography of a blank substrate and substrate coated with Na_2MoO_4. (b-i) Optical microscopy images of the marked position in (a) (Scale Bar: 100 μm). The MoS_2 flakes on the blank substrate indicate the diffusion of Na_2MoO_4.

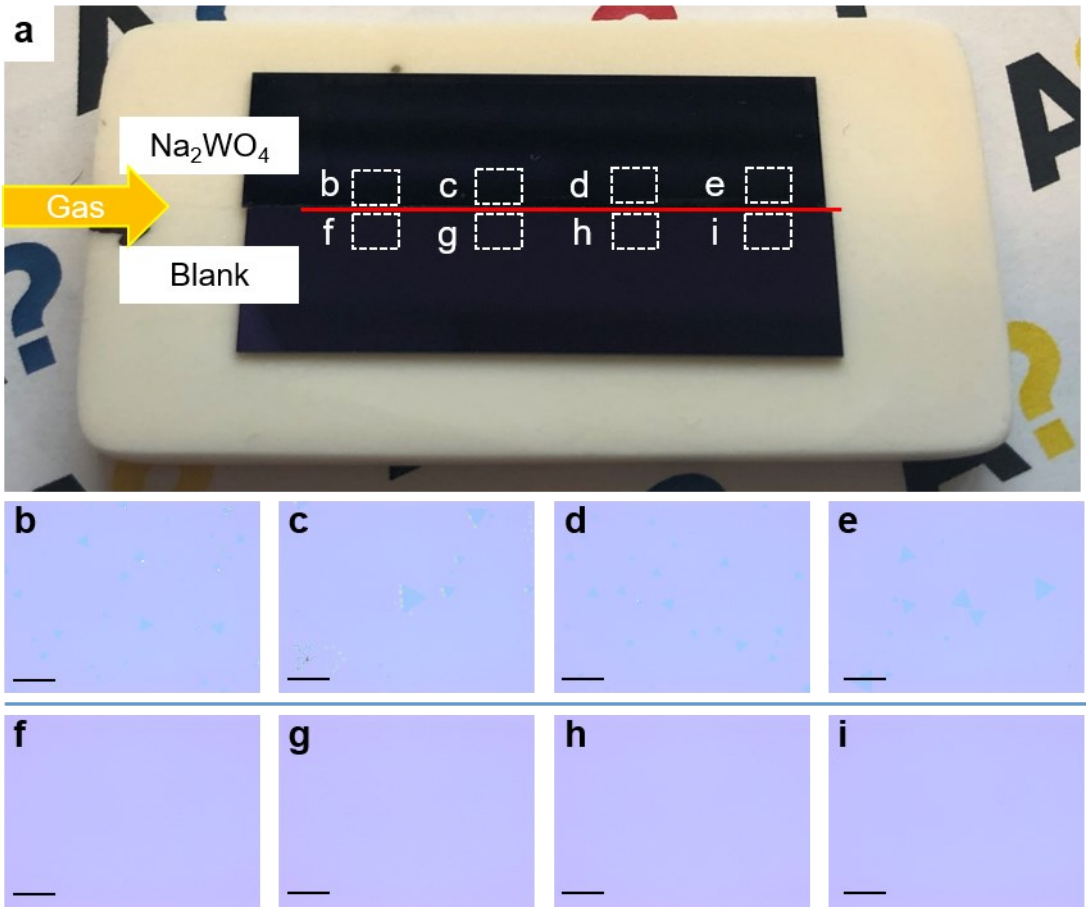

Figure S7. Control experiment of Na_2WO_4 diffusion. (a) Photography of a blank substrate and substrate coated with Na_2WO_4. (b-i) Optical microscopy images of the marked position in (a) (Scale Bar: 100 μm). No WS_2 flakes on the blank substrate indicate no diffusion of Na_2WO_4.

Growth result of the mixture Na_2MoO_4 and Na_2WO_4

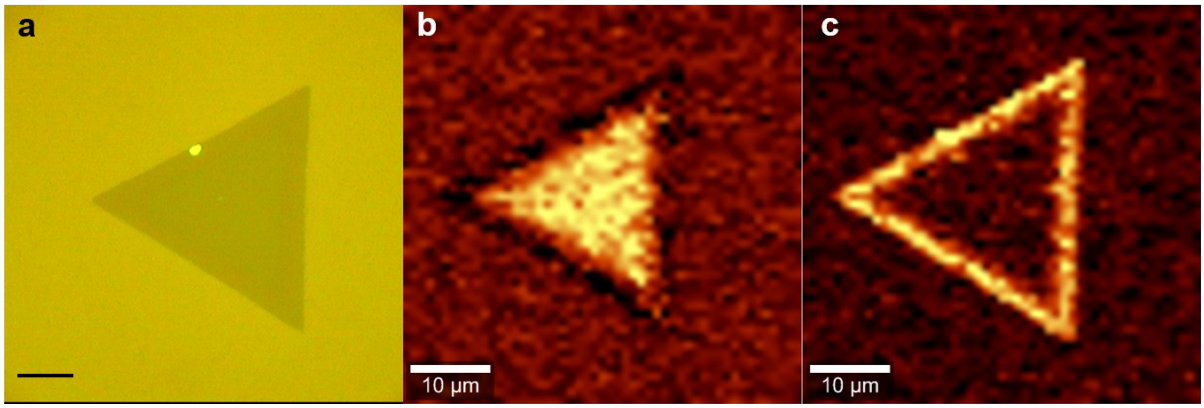

Figure S8. Growth result of the mixture of Na_2MoO_4 and Na_2WO_4 as precursors. (a) Optical image of a flake (Scale Bar, 10 μm). (b-c) Raman mapping at (b) 385 cm^{-1} (MoS_2) and (c) 351 cm^{-1} (WS_2), respectively. Clearly, the mixture of Na_2MoO_4 and Na_2WO_4 as precursors forms a lateral heterostructure instead of the anti-pyramid vertical heterostructure.

References

(1) Hsu, W.-T.; Zhao, Z.-A.; Li, L.-J.; Chen, C.-H.; Chiu, M.-H.; Chang, P.-S.; Chou, Y.-C.; Chang, W.-H. Second harmonic generation from artificially stacked transition metal dichalcogenide twisted bilayers. *ACS Nano* 2014, **8**, 2951-2958.
(2) Autere, A.; Jussila, H.; Dai, Y.; Wang, Y.; Lipsanen, H.; Sun, Z. Nonlinear optics with 2D layered materials. *Adv. Mater.* 2018, **30**, 1705963.
(3) Choi, S.H.; Kim, Y.J.; Yang, W.; Kim, K.K. Alkali Metal-Assisted Growth of Single-Layer Molybdenum Disulfide. *J Korean Phys. Soc.* 2019, **74**, 1032-1038